Chinese Chemical Letters 31 (2020) 517–520

Contents lists available at ScienceDirect

Chinese Chemical Letters

journal homepage: www.elsevier.com/locate/cclet

Communication

One-dimensional HKUST-1 nanobelts from Cu nanowires

Qin Li[a,b], Wei Zhu[a,b,*], Yuebin Lian[a,b], Yang Peng[a,b], Zhao Deng[a,b,*]

[a] Soochow Institute for Energy and Materials Innovations, College of Energy, Soochow University, Suzhou 215006, China
[b] Key Laboratory of Advanced Carbon Materials and Wearable Energy Technologies of Jiangsu Province, Soochow University, Suzhou 215006, China

ARTICLE INFO

Article history:
Received 21 March 2019
Received in revised form 9 April 2019
Accepted 6 May 2019
Available online 8 May 2019

Keywords:
Metal-organic frameworks
Nanobelts
Inorganic materials
Self-assembly
One-dimensional structure

ABSTRACT

The controllable synthesis of one-dimensional (1D) structural morphology of metal-organic frameworks (MOFs) is significant for its application in catalysis, sense and gas separation. In this communication, we report a simple and moderate synthetic strategy to obtain uniform HKUST-1 nanobelts (NBs) by using copper nanowires (Cu NWs) as a metal source as well as a template. The control experiments showed that synergy between metal dissolution rate and crystal formation plays a key role in the formation of nanobelts. Our study represents an attractive synthetic strategy of 1D MOFs-based material for applications.

Metal-organic frameworks (MOFs), a class of porous crystal materials with high surface and ordered channel structure [1], have been widely studied in many fields, such as gas separation and storage [2], catalysis [3,4], sensors [5,6], drug delivery [7], wastewater treatment [8]. Typically the structure of most MOFs are three-dimensional, and the precise control the low-dimensional microstructure of MOFs usually requires additional additives as structure guide or template agent [9]. So in recent years, the research about morphological control of low-dimensional MOFs is common occurrence.

Among these colorful MOFs materials, 1D structures such as rods, wires, tubes and belts have always been a research hotspot due to their excellent utilization potentiality in electronic or optoelectronic devices [10–12]. So far, the 1D MOFs materials is mainly focused on two types: one is MOFs-based composite structure, in which the MOFs particles are combined with an one-dimensional materials (such as metal and semiconductor) to form the package or core-shell structure [13]. For example, Liu *et al.* first reported a Si NWs/MOF hybrid structure of MOF-199 wrapped on the -COOH modified silicon nanowires through step-by-step growth, they found that the interaction of the MOFs coordinating groups with the Si NWs surface functional group is crucial for the growth of the hybrid materials [14]. Zhan *et al.* used the ZnO array as a pecursor material to *in-situ* growth ZIF-8. After adjusted the corresponding parameters of reaction temperature, ligand concentration and reaction time, they successfully prepared a core-shell structure of ZnO@ZIF-8 nanorods arrays, which displayed distinct photoelectrochemical response to H_2O_2 and ascorbic acid [15]. Furthermore, Zhang *et al.* prepared a 1D package structure of CuNWs@ZIF-8 by microwave heating method, and the composite material exhibited an excellent performance in hydrogen conversion with the hydrolysis of ammonia borane [16]. From the above, it can be seen that reasonable packaging of one-dimensional materials by MOFs can effectively improve their properties. The other method for the preparation of 1D MOFs materials is using end-capping reagent or template. For example, Luz *et al.* reported a one-step synthetic strategy for Cu@Cu-MOF-74 rods, they discussed in detail the effects of various factors in the reaction on the structure, including reaction time, the ligand-to-Cu molar ratio, solvent and reaction temperature [17]. While Zou *et al.* reported the fabrication of single-crystal MOF nanotubes *via* an amorphous MOF-mediated recrystallization approach. The obtained MOF nanotubes can be used to separate large molecules such as rhodamine B [18]. Zhang *et al.* used ultrathin tellurium nanowires as templates to direct growing ZIF-8 nanofibers, the derived porous doped carbon nanofibers exhibited excellent electrocatalytic performance for oxygen reduction reaction [19]. Furthermore, Pachfule *et al.* synthesized MOF-74 rods in the presence of salicylic acid as a modulator. After heat treatment of the MOFs rods, the obtained carbon nanorods exhibited excellent performance in supercapacitor electrodes [20]. Although both of these two strategies can construct a good one-dimensional structure of MOFs, it is still a significant challenge to conduct dynamic control of one-dimensional MOFs without any assistance.

Herein, we demonstrate a strategy for the synthesis of 1D MOFs (HKUST-1 nanobelts) from Cu NWs (ligand-free) by a traditional hydrothermal method. The Cu NWs act as a copper source and

* Corresponding authors at: Soochow Institute for Energy and Materials Innovations, College of Energy, Soochow University, Suzhou 215006, China.
E-mail addresses: zhuw@suda.edu.cn (W. Zhu), zdeng@suda.edu.cn (Z. Deng).

https://doi.org/10.1016/j.cclet.2019.05.005
1001-8417/

template during the transformation process of HKUST-1 nanobelts, and the molar ratio of Cu NWs/H_3BTC and the reaction time play important roles in the morphology of the final products. Finally, a possible reaction mechanism is proposed based on the kinetic process. This work provides a strategy to future design and synthesize 1D structure of MOFs and metals@MOFs hybrids.

The XRD of HKUST-1 nanobelts was shown in Fig. 1a. Comparing with the particles, the HKUST-1 nanobelts exhibit a same XRD patterns, confirming both of the HKUST-1 nanobelts and particles have the same structure. Although the (222) plane is still a dominant crystal surface (Fig. S1 in Supporting information), the peak at around 2θ value of 9°, which can be assigned to (220) planes, shows a stronger peak intensity in HKUST-1 nanobelts, indicating the exposure of the crystal surface is enhanced [21,22]. From the FESEM images of Cu NWs, HKUST-1 nanobelts (Figs. 1b and c), it can be seen that the Cu NWs exhibited extremely smooth surface but with some Cu nanoparticles, which is inevitable in our preparation [23]. But after the Cu NWs react with H_3BTC under 80 °C for 20 h, there is no Cu NWs but uniform HKUST-1 nanobelts can be obtained from the products, and the surface of nanobelts remain smooth with a width of about 300 nm.

To further study the microscopic property of the HKUST-1 nanobelts, the atomic force microscope (AFM) was used to characterize the surface property of the nanobelts. From the AFM images, it can be seen that the width of Cu NWs is 100 nm with a thickness of 50 nm (Fig. 1d), and there is no obvious defect on the surface. However, although the nanobelts are inherited the smooth surface property of the Cu NWs, the width is up to 300 nm and the thickness reached 170 nm (Fig. 1e), which are both larger than the Cu NWs. In addition, the average length of the belts could reach up to about 60 μm, which is twice longer than the Cu NW with an average length of 30 μm, indicating the HKUST-1 nanobelts may be grown by a process of Cu NWs surface dissolving and MOFs self-assembling growth. Due to the high aspect ratio (1:100) with the nano-sized diameter, the HKUST-1 nanobelts exhibited a lower thermal stability than the HKUST-1 polyhedrons from the thermogravimetric analysis (Fig. S2 in Supporting information), and it can be calculated out that the molar ratio of Cu/H_3BTC of the nanobelts is about 3:2 from the mass loss of TGA, which is consistent with the theoretical value of HKUST-1. Furthermore, it should be worth noting that the mass loss of the nanobelts before 250 °C is much less than HKUST-1 nanoparticles, indicating that the guest molecules adsorbed in nanobelts is lower than particles, which is in agreement with the lower BET of nanobelts (161 m^2/g) than the particles (1217 m^2/g) (Fig. S3 in Supporting information).

To better understanding the structural transformation mechanism of HKUST-1 nanobelts from Cu NWs, we first investigated the influence of the concentration of H_3BTC. The SEM images of different mole ratios of Cu/H_3BTC are shown in Fig. 2 and Fig. S4 (Supporting information) corresponding to different size of scales. It can been seen that the surface of Cu NWs are rugged after hydrothermal reaction without the organic ligands, and the characteristic peak of Cu_2O can be found at $2\theta = 36.6°$, 42.5° and 61.6° from the XRD characterization (Fig. S5 in Supporting information), indicating the surface of the Cu NWs has been oxidized to Cu_2O. When the H_3BTC is added, a lot of particles of HKUST-1 are present in the products, and at the same time, a layer of HKUST-1 particles appeared on the surface of the nanowires (Fig. 2b). With the increase of ligand addition, the more particles were produced. However, when the molar ratio of Cu/H_3BTC reached 1:40, only nanobelts can be found in the final products (Fig. 2g), and its structure was verified by XRD (Fig. S6). More organic ligands do not affect the formation of nanobelts (Fig. 2h).

Next, we investigated the influence of the reaction time with a fixed ratio of Cu to H_3BTC at 1:40. The SEM images of different reaction time are shown in Fig. 3. It can been seen that when the hydrothermal reaction is 2 h, the thin layer of HKUST-1 appeared on the copper nanowire, which can be confirmed by XRD (Fig. 3a and Fig. S7 in Supporting information). With the prolonging of reaction time, the HKUST-1 layer on the surface of copper nanowires becomes thicker, but the crystallinity is getting better and better. Finally, all of the Cu NWs are transformed into nanobelts at 20 h. However, when use Cu^{2+} as the Cu source, there is only HKUST-1 particles in the final products (Fig. S8 in Supporting information).

On the basis of the above observations, a formation mechanism can be proposed (Scheme 1). In the whole process, the Cu NWs play roles of both Cu source and structure-directing agent. First, the Cu NWs are oxidized by the dissolved O_2 to form Cu_2O ($4Cu + O_2 \rightarrow 2Cu_2O$). However, the Cu_2O is not stable in the acid solution with disproportionation ($Cu_2O + 2H^+ \rightarrow Cu^{2+} + Cu + H_2O$). Once the Cu^{2+} formed and dissociated into the solution, the H_3BTC will immediately coordinate with it to form coordination polymer of

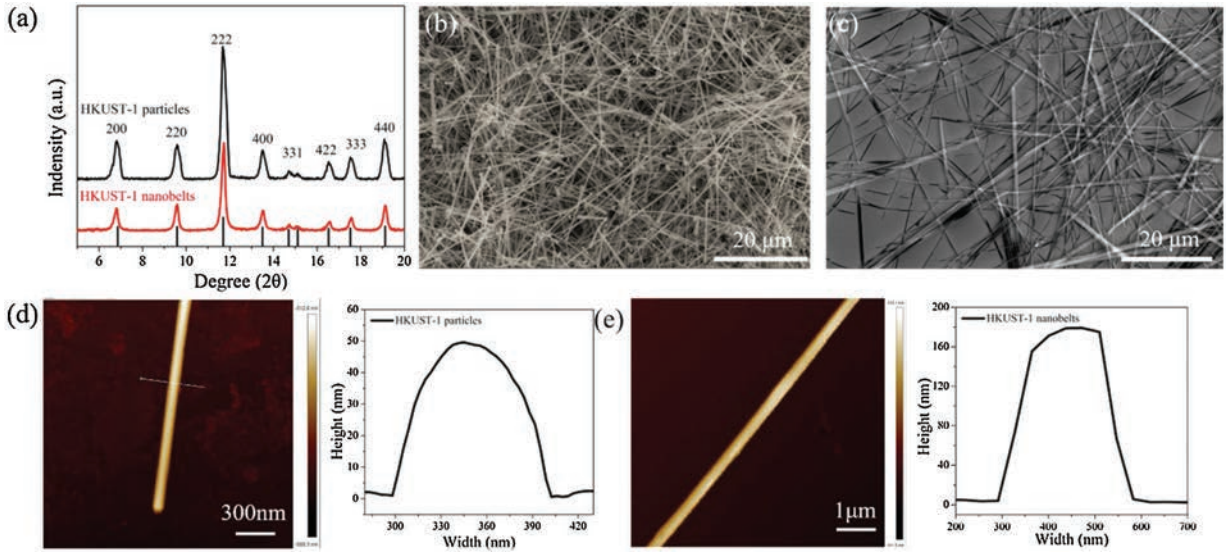

Fig. 1. (a) XRD patterns of HKUST-1 particles and HKUST-1 nanobelts; SEM images of (b) CuNWs and (c) HKUST-1 nanobelts; AFM image of (d) CuNWs and (e) HKUST-1 nanobelts.

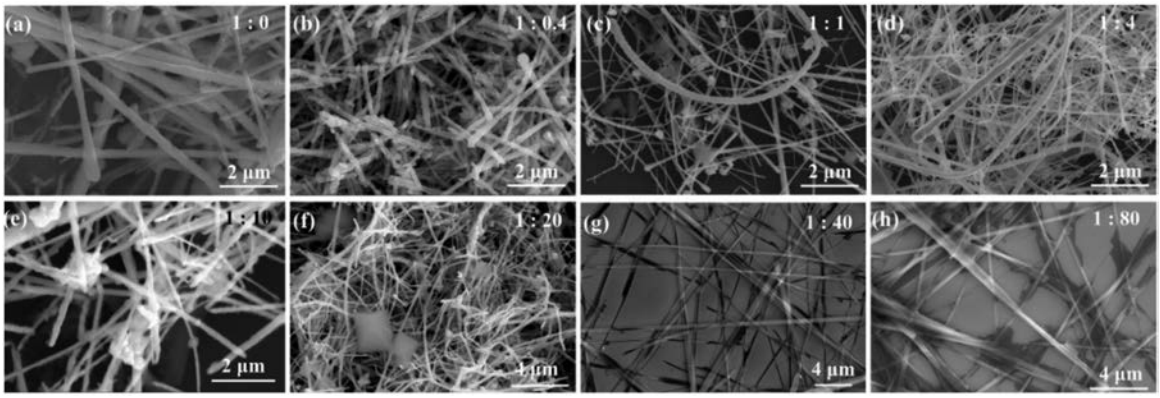

Fig. 2. SEM images of the products at different ligand concentration with small scale, the mass ratio of Cu NWs and H_3BTC are (a) 1:0, (b) 1:0.4, (c) 1:1, (d) 1:4, (e) 1:10, (f) 1:20, (g) 1:40, (h) 1:80.

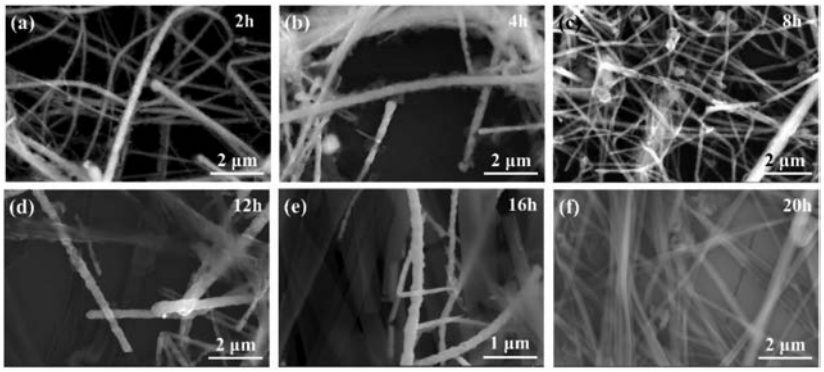

Fig. 3. SEM images of the products at different time of (a) 2 h, (b) 4 h, (c) 8 h, (d) 12 h, (e) 16 h and (f) 20 h.

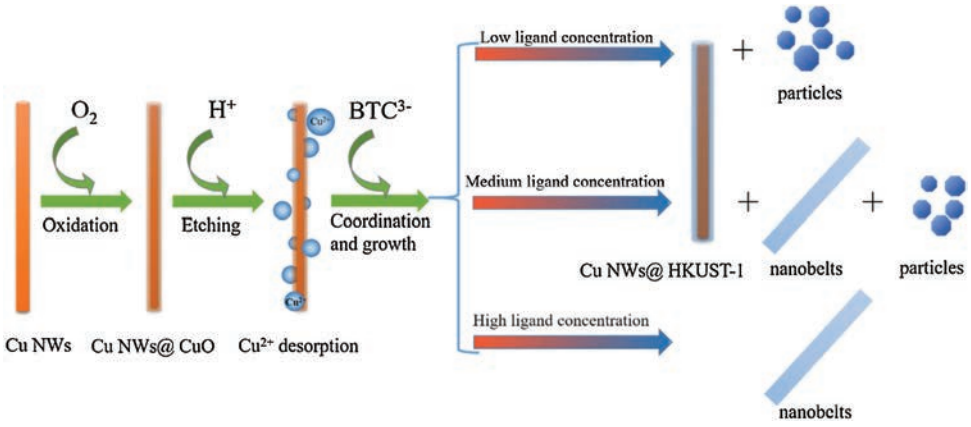

Scheme 1. reaction mechanism of CuNWs @ HKUST-1 and HKUST-1 nanobelts.

HKUST-1. So the balance between the release rate of Cu^{2+} and heterogeneous nucleate rate of HKUST-1 is the key for the formation of HKUST-1 nanobelts. When the concentration of the ligand is low, the excess Cu^{2+} will diffuse into the solution and coordinate with the BTC anion to form HKUST-1 with anisotropic growth. However, when the concentration of ligand is high enough, the ligand would coordinate with Cu^{2+} as soon as the Cu^{2+} diffused out from the Cu NWs, and then nucleated and grown along the MOFs that is wrapped on the Cu NWs. In this case, Cu NWs play the roles of Cu source and structure-directing agent. Due to the porous structure of the MOFs, the O_2 and H^+ could still etching Cu NWs though the channels of the MOFs, and the Cu^{2+} could diffused out though the pores. The pore size of different crystal planes will affect the mass transfer of Cu^{2+} and organic ligand, as well as the O_2, which will affect the growth rate of the crystal direction, resulting in the formation of the nanobelts with high aspect ratio.

In summary, we successfully synthesized the HKUST-1 nanobelts by one-step hydrothermal method from Cu NWs. The novel structural transformation process of Cu NWs to HKUST-1 nanobelts is attributed to the template dissolving and self-assembling process with coordination reaction. This study is crucial to develop the nanotechnology of design for MOFs-based one-dimensional

materials, which represent an attractive synthetic strategy of 1D MOFs-based material for applications.

Acknowledgments

This work was supported by the National Natural Science Foundation of China (No. 21701118), the Natural Science Foundation of Jiangsu Province (Nos. BK20161209 and BK20160323), Natural Science Research Project of Jiangsu Higher Education Institutions (No. 18KJA480004) and Priority Academic Program Development (PAPD) of Jiangsu Higher Education Institutions. We also extend our sincere appreciation to the support by Suzhou Key Laboratory for Advanced Carbon Materials and Wearable Energy Technologies, Suzhou 215006, China.

Appendix A. Supplementary data

Supplementary material related to this article can be found, in the online version, at doi:https://doi.org/10.1016/j.cclet.2019.05.005.

References

[1] M.J. Rosseinsky, Microporous Mesoporous Mater. 73 (2004) 15–30.
[2] Y. Lin, C. Kong, Q. Zhang, L. Chen, Adv. Energy Mater. 7 (2017) 1601296.
[3] A. Dhakshinamoorthy, A.M. Asiri, H. Garcia, Angew. Chem. Int. Ed. 55 (2016) 5414–5445.
[4] C.C. Wang, Y.Q. Zhang, J. Li, P. Wang, J. Mol. Struct. 1083 (2015) 127–136.
[5] I. Stassen, N. Burtch, A. Talin, et al., Chem. Soc. Rev. 46 (2017) 3185–3241.
[6] F.Y. Yi, D. Chen, M.K. Wu, L. Han, H.L. Jiang, ChemPlusChem 81 (2016) 675–690.
[7] M.X. Wu, Y.W. Yang, Adv. Mater. 29 (2017) 1606134.
[8] Q. Fu, L. Wen, L. Zhang, Y. Yang, H. Zhang, ACS Appl. Mater. Inter. 9 (2017) 33979–33988.
[9] K. Okada, R. Ricco, Y. Tokudome, et al., Adv. Funct. Mater. 24 (2014) 1969–1977.
[10] J.W. Jiang, T. Rabczuk, Appl. Phys. Lett. 102 (2013) 123104.
[11] J.W. Jiang, N. Yang, B.S. Wang, T. Rabczuk, Nano Lett. 13 (2013) 1670–1674.
[12] N.P. Dasgupta, J. Sun, C. Liu, et al., Adv. Mater. 26 (2014) 2137–2184.
[13] V. André, F. Galego, M. Martins, Cryst. Growth Des. 18 (2018) 2067–2081.
[14] N. Liu, Y. Yao, J.J. Cha, et al., Nano Res. 5 (2011) 109–116.
[15] W.W. Zhan, Q. Kuang, J.Z. Zhou, et al., J. Am. Chem. Soc. 135 (2013) 1926–1933.
[16] D. Zhang, P. Liu, S. Xiao, et al., Nanoscale 8 (2016) 7749–7754.
[17] I. Luz, A. Loiudice, D.T. Sun, W.L. Queen, R. Buonsanti, Chem. Mater. 28 (2016) 3839–3849.
[18] L. Zou, C.C. Hou, Z. Liu, H. Pang, Q. Xu, J. Am. Chem. Soc. 140 (2018) 15393–15401.
[19] W. Zhang, Z.Y. Wu, H.L. Jiang, S.H. Yu, J. Am. Chem. Soc. 136 (2014) 14385–14388.
[20] P. Pachfule, D. Shinde, M. Majumder, Q. Xu, Nat. Chem. 8 (2016) 718–724.
[21] B. Mortazavi, M. Shahrokhi, M. Makaremi, G. Cuniberti, T. Rabczuk, Mater. Today Energy 10 (2018) 336–342.
[22] B. Mortazavi, M. Shahrokhi, T. Hussain, X. Zhuang, T. Rabczuk, Appl. Mater. Today 15 (2019) 405–415.
[23] S. Ye, I.E. Stewart, Z. Chen, et al., Accounts Chem. Res. 49 (2016) 442–451.